A Fast Recursive Algorithm for the Estimation of Frequency, Amplitude, and Phase of Noisy Sinusoid

P. K. Dash, *Life Senior Member, IEEE*, and Shazia Hasan, *Member, IEEE*

***Abstract*—This paper presents an adaptive method for tracking the amplitude, phase, and frequency of a time-varying sinusoid in white noise. Although the conventional techniques like adaptive linear elements and discrete or fast Fourier transforms are still widely used in many applications, their accuracy and convergence speed pose serious limitations under sudden supply frequency drift, fundamental amplitude, or phase variations. This paper, therefore, proposes a fast and low-complexity multiobjective Gauss–Newton algorithm for estimating the fundamental phasor and frequency of the power signal instantly and accurately. Further, the learning parameters in the proposed algorithm are tuned iteratively to provide faster convergence and better accuracy. The proposed method can also be extended to include time-varying harmonics and interharmonics mixed with noise of low signal-to-noise ratio with a great degree of accuracy. Numerical and experimental results are presented in support of the effectiveness of the new approach.**

***Index Terms*—Amplitude and phase estimation, Gauss–Newton method, linear prediction, Newton method, sinusoid.**

I. Introduction

SINUSOIDAL parameter estimation from noisy measurements has many applications in sonar, radar, and digital communications, biomedical engineering, and power systems. In the case of power networks, simultaneous estimation of the power signal parameters like the amplitude, phase, and frequency is required not only for the control and protection but also for the efficient operation of distribution generation systems in a microgrid environment using microcontrollers [1]. Further, the recent introduction of phasor measurement units for wide area control and protection of power networks will require efficient and accurate estimation of fundamental signal parameters. The electrical parameter measurement of a power signal is relatively a straightforward matter, as long as the frequency of the signal is not time varying. However, if the frequency varies, the parameters of the power system network cannot be estimated accurately, and this is further complicated due to the presence of harmonics, interharmonics, and noise in the signal. A similar scenario also prevails in the case of low-frequency signals that occur in sonar and radar communications and mechanical systems [2]. Thus, there is a need for an algorithm that should perform consistently for a signal with time-varying amplitude, phase, and frequency harmonics in the presence of noise. Until today, there are few algorithms that can achieve accurate results in all these aspects. Among the three signal parameters, frequency is one of the most important one, and once it is measured accurately, estimation of other parameters like amplitude and phase is relatively easy. The most widely used methods for frequency estimation include the following: zero crossing technique [3], discrete Fourier transform (DFT) and fast Fourier transform (FFT) [4], adaptive linear elements (ADALINEs) using least mean squares technique (LMS) [5] and recursive least square (RLS) [6], adaptive notch filter [7], Newton's type algorithms [8], supervised Gauss–Newton algorithms [9], Kalman filters [10], [11], neural methods [12], [13], wavelet transform [14], linear prediction (LP) methods [15], [16], and maximum likelihood estimates [17].

As is well known, both DFT and FFT methods suffer from leakage and picket fence effects and give erroneous results for time-varying signals and, particularly, when the sampling frequency is not an integer multiple of the fundamental frequency. All the algorithms listed earlier are computationally intensive and do not produce accurate results under time-varying situations. The LMS and RLS algorithms are widely used as the former one is simple and can be used to accurately estimate the amplitude and phase of a sinusoid and also the harmonics, if they are present in the signal, provided that the fundamental frequency is known *a priori*. In this case, change of frequency can be estimated separately taking three consecutive samples of the signal. The recursive RLS produces accurate estimate of the parameters of the signal but is computationally more rigorous, and for harmonic estimation, it needs matrix inversion at each time step. LP algorithms produce accurate estimate of signal frequency of stationary signal or multiple sinusoids and need matrix inversion at every iteration leading to complexity.

In the recently proposed modified Newton method [18], the frequency of single or multiple sinusoids is computed using a linear predictor formulation and subsequent optimization. This method, however, is only applicable to frequency estimation but not for amplitude and phase estimation simultaneously. On the other hand, the recursive Gauss–Newton (RGN) algorithm [19] assumes the frequency of the sinusoidal signal *a priori* and computes the amplitude and phase of the signal only. Other methods include differentiation filter, iterative-loop approaching method, simple recursive methods, etc. [20]–[25]. Thus, keeping the objective as stated in the beginning, there is a need for an overall approach for the estimation of the frequency,

Manuscript received March 11, 2010; revised June 24, 2010, September 21, 2010, and December 21, 2010; accepted January 25, 2011. Date of publication February 24, 2011; date of current version August 30, 2011.

P. K. Dash is with Siksha O Anusandhan University, Bhubaneswar 751030, India (e-mail: pkdash.india@gmail.com).

S. Hasan is with the Institute of Technical Education and Research, Siksha O Anusandhan University, Bhubaneswar 751030, India (e-mail: shasan_uce@rediffmail.com).

Color versions of one or more of the figures in this paper are available online at http://ieeexplore.ieee.org.

Digital Object Identifier 10.1109/TIE.2011.2119450

amplitude, and phase of a sinusoid simultaneously; this paper presents a multiobjective Gauss–Newton (MGN) algorithm to simultaneously estimate the amplitude, phase, and frequency of a sinusoid.

The major contribution of this paper is to simplify the RGN method to reduce the computational complexity and produce a better accuracy in estimation under nonstationary condition using two objective functions for error minimization. Here, the term multiobjective means that, for amplitude and phase, one objective function is chosen for error minimization, while for frequency estimation, another objective function comprising of three consecutive samples and a weighted error cost function is used unlike the Newton method [18]. Further, the forgetting factors of the algorithm are tuned iteratively for better estimation. Section III-A and B develop the new integrated MGN method which is applied to estimate the power signal parameters as well as low- and high-frequency signal parameters accurately, which occur in other dynamic and communication systems. Section III-C presents the performance analysis, while in Section IV, simulation and experimental results are presented for evaluating its accuracy and efficiency in the presence of signal distortion. Finally, conclusion is drawn in Section V.

II. Problem Formulation

The problem of sinusoidal parameter estimation is formulated for discrete-time noisy measurements as

$$y(k) = s(k) + v(k), \qquad k = 0, 1, 2, \ldots, N-1 \tag{1}$$

$$s(k) = A(k) \sin\left(w(k)k + \phi(k)\right) \tag{2}$$

where A, w, and ϕ are unknown values that denote the amplitude, frequency, and phase of a real valued sinusoid, respectively, while $v(k)$ is an additive white noise with unknown variance σ_v^2. The proposed algorithm for the estimation of frequency, amplitude, and phase of the sinusoid is presented hereinafter.

III. MGN

A. Frequency Estimation

An error objective function is formulated using consecutive $2R$ samples (R is the number of sinusoids in the signal) for estimating the time-varying frequency of the signal in (2). In this method, the frequency of the signal is estimated using the properties of a linear predictor, and then, the amplitude and phase of the signal are estimated using the RGN approach. It has been shown in [18] that $s(k)$ can be uniquely expressed as a linear combination of its previous $2R$ samples as

$$s(k) = -\sum_{i=1}^{2R} a_i s(k-i) \tag{3}$$

where a_i is referred to as linear prediction coefficients. The relationship between w and a_i is given in [13] as

$$\sum_{i=0}^{2R} a_i \exp(-jwi) = 0, \qquad a_i = a_{2R-i}; \quad i = 0, 1, 2, \ldots, R. \tag{4}$$

In the aforementioned equation, a_0 is chosen as one, and the signal estimation error is defined as

$$e_w(k) = \sum_{i=0}^{R-1} \widetilde{a}_i \left(y(k-i) + y(k-2R+i)\right) + \widetilde{a}_R y(k-R) \tag{5}$$

where $\widetilde{a}_i$ denotes the optimized value of a_i; here, $\widetilde{a}_0$ may not be fixed to unity. For error minimization, an exponentially weighted cost function is used as follows:

$$\varepsilon_1(k) = \sum_{i=0}^{k} \lambda_1^{k-i} e_w^2(i) \tag{6}$$

where $0 < \lambda_1 \leq 1$ is the forgetting factor. For the estimation of frequency of a single sinusoid ($R = 1$) according to (4), the linear predictor coefficients required are a_0, a_1, and $a_2 (a_2 = a_0)$. In this case, (5) is rewritten with $R = 1$ as

$$e_W(k) = \widetilde{a}_0 \left(y(k) + y(k-2)\right) + \widetilde{a}_1 y(k-1). \tag{7}$$

Hence, the parameter vector to be estimated is given by $\widetilde{\theta}(k) = [\widetilde{a}_0 \quad \widetilde{a}_1]^{\mathrm{T}}$. Since, for time-varying frequency, e_w is not linear in $\widetilde{a}_0$ and $\widetilde{a}_1$ due to the time-varying nature of the signal, conventional RLS [6] algorithm cannot be applied to minimize (6). Thus, an RGN method [19] is used to minimize (6), and the updating equation for sinusoidal parameter estimation under noisy condition is as follows:

$$\widetilde{\theta}(k) = \widetilde{\theta}(k-1) - H^{-1}(k)\psi(k)e_w(k) \tag{8}$$

$$H(k) = \sum_{i=0}^{k} \lambda_1^{k-i} \psi(i)\psi^T(i) \tag{9}$$

where the gradient vector ψ and the Hessian matrix $H(k)$ [19] are obtained after some simple manipulation as (10) and (11), shown at the bottom of the page.

To compute the inverse Hessian matrix, one can directly use the matrix inverse lemma at the cost of high computational

$$\psi(k) = \frac{\partial e_w(k)}{\partial \widetilde{\theta}} = \begin{bmatrix} y(k) + y(k-2) \\ y(k-1) \end{bmatrix} \tag{10}$$

$$H(k) = \sum_{i=0}^{k} \lambda_1^{k-i} \begin{bmatrix} \left(y(k) + y(k-2)\right)^2 & \left(y(k) + y(k-2)\right)\left(y(k-1)\right) \\ \left(y(k) + y(k-2)\right)\left(y(k-1)\right) & \left(y(k-1)\right)^2 \end{bmatrix} \tag{11}$$

complexity, and thus, an approximation is performed for fast computation of the frequency iteratively. Assuming that w is not near to zero or π, $H(k)$ can be approximated as (12), shown at the bottom of the page.

The inverse of the Hessian matrix can be easily calculated as (13), shown at the bottom of the page, where

$$c(k) = \frac{1-\lambda_1^{k+1}}{2(1-\lambda_1)}. \tag{14}$$

We can observe that $c(k)$ can be computed recursively as

$$c(k) = \lambda_1 c(k-1) + 1/2. \tag{15}$$

Further, by putting (13) and (14) into (8), the following equations are obtained:

$$\begin{aligned}\widetilde{a}_0(k) =& \widetilde{a}_0(k-1) - e_w(k)/4c(k)A\cos(w) \\ &\times \sin\left(w(k-1)+\phi(k-1)\right) \qquad (16)\\ \widetilde{a}_1(k) =& \widetilde{a}_1(k-1) - e_w(k)/2c(k)A \\ &\times \sin\left(w(k-1)+\phi(k-1)\right). \qquad (17)\end{aligned}$$

After estimating $\widetilde{a}_0$ and $\widetilde{a}_1$, the frequency of the sinusoid is computed as $\cos^{-1}(-\widetilde{a}_1/2)$.

B. Amplitude and Phase Estimation

Once the frequency is estimated, the amplitude and phase of the signal are calculated using the RGN method in the same iteration. For calculating the amplitude and phase of a sinusoid, let the parameter vector be $\theta(k) = [A(k) \quad \phi(k)]^{\mathrm{T}}$ and its estimate be $\hat{\theta}(k) = [\hat{A}(k) \quad \hat{\phi}(k)]^{\mathrm{T}}$. Using $\hat{\theta}(k-1)$, the estimate of $y(k)$ at time k is computed as

$$\hat{y}(k) = \hat{A}(k-1)\sin\left(wk + \hat{\phi}(k-1)\right). \tag{18}$$

The *a priori* estimation error at time k is given as

$$e_\theta(k) = y(k) - \hat{A}(k-1)\sin\left(wk+\hat{\phi}(k-1)\right) \tag{19}$$

and a similar kind of cost function is taken as in (6)

$$\varepsilon_2(k) = \sum_{i=0}^{k} \lambda_2^{k-i} e_\theta^2(i) \tag{20}$$

where $0 < \lambda_2 \leq 1$ is the forgetting factor. In this case, RGN method is also used to minimize (20) in a similar way as mentioned earlier. The gradient vector is given by

$$\psi(k) = \frac{\partial e_\theta(k)}{\partial \hat{\theta}} = \begin{bmatrix} -\sin\left(wk+\hat{\phi}(k-1)\right) \\ -\hat{A}(k-1)\cos\left(wk+\hat{\phi}(k-1)\right)\end{bmatrix} \tag{21}$$

and the Hessian matrix is obtained as (22), shown at the bottom of the page.

In a similar manner, for the frequency case, the Hessian matrix in (22) is approximated as

$$\begin{aligned}H(k) &= \sum_{i=0}^{k} \lambda_2^{k-i} \begin{bmatrix} 1/2 & 0 \\ 0 & \hat{A}^2(k-1)/2\end{bmatrix} \\ &= \frac{1-\lambda_2^{k+1}}{2(1-\lambda_2)} \begin{bmatrix} 1 & 0 \\ 0 & \hat{A}^2(k-1)\end{bmatrix}\end{aligned} \tag{23}$$

and the inverse Hessian matrix can be easily computed as

$$H^{-1}(k) = \begin{bmatrix} 1/c(k) & 0 \\ 0 & 1/\hat{A}^2(k-1)c(k)\end{bmatrix} \tag{24}$$

where $c(k)$ is the same as in (14) with forgetting factor λ_2.

Further, by putting (24) and (14) into (8), the amplitude and phase are calculated as

$$\begin{aligned}\hat{A}(k) =& \hat{A}(k-1) + \sin\left(\hat{w}(k-1)k + \hat{\phi}(k-1)\right) \\ &\times e_\theta(k)/c(k) \qquad (25)\\ \hat{\phi}(k) =& \hat{\phi}(k-1) + \cos\left(\hat{w}(k-1)k + \hat{\phi}(k-1)\right) \\ &\times e_\theta(k)/\left(\hat{A}(k-1)c(k)\right). \qquad (26)\end{aligned}$$

$$H(k) = \frac{1-\lambda_1^{k+1}}{1-\lambda_1} \begin{bmatrix} 4A^2\cos^2(w)\sin^2\left(w(k-1)+\phi(k-1)\right) & 0 \\ 0 & A^2\sin^2\left(w(k-1)+\phi(k-1)\right)\end{bmatrix} \tag{12}$$

$$H^{-1}(k) = \begin{bmatrix} 1/8c(k)A^2\cos^2(w)\sin^2\left(w(k-1)+\phi(k-1)\right) & 0 \\ 0 & 1/2c(k)A^2\sin^2\left(w(k-1)+\phi(k-1)\right)\end{bmatrix} \tag{13}$$

$$H(k) = \sum_{i=0}^{k} \lambda_2^{k-i} \begin{bmatrix} \sin^2\left(w+\hat{\phi}(k-1)\right) & \hat{A}(k-1)\sin\left(2\left(wi+\hat{\phi}(k-1)\right)\right)/2 \\ \hat{A}(k-1)\sin\left(2\left(wi+\hat{\phi}(k-1)\right)\right)/2 & \hat{A}^2(k-1)\cos^2\left(wi+\hat{\phi}(k-1)\right)\end{bmatrix} \tag{22}$$

From the above-mentioned equations, we can observe that the forgetting factors λ_1 and λ_2 influence the estimation process. The initial values can be any arbitrary value within the range $0 < \lambda < 1$. When the signal is contaminated with high random noise, forgetting factor close to 0.5 results in faster convergence but increased sensitivity to noise. However, using forgetting factor close to one (e.g., $\lambda = 0.99$) results in slow convergence but better noise rejection property. Motivated by these aspects, a number of variable forgetting factor RLS algorithms have been developed [26]. The *a priori* estimation error is given by (19), and the *a posteriori* estimation function is given as

$$\varsigma(k) = y(k) - \hat{A}(k)\sin\left(wk + \hat{\phi}(k)\right). \tag{27}$$

To make the update equation stable, assume that

$$E\left(\varsigma^2(k)\right) = \sigma_v^2 \tag{28}$$

where σ_v^2 is the power of the system noise.

Solving for the aforementioned condition, a time-dependent variable forgetting factor can be generated as

$$\lambda_k = \frac{\sigma_b(k)\sigma_v}{\sigma_e(k) - \sigma_v} \tag{29}$$

where $E(b^2(k)) = \sigma_b^2(k)$, $E(e_\theta(k)) = \sigma_e^2(k)$ which is the power of error signal, and $b(k) = \psi(k)^T H(k)\psi(k)$. The power estimates are computed iteratively as

$$\hat{\sigma}_e^2(k) = \tau\hat{\sigma}_e^2(k-1) + (1-\tau)e_\theta^2(k) \tag{30}$$

$$\hat{\sigma}_b^2(k) = \tau\hat{\sigma}_b^2(k-1) + (1-\tau)b^2(k) \tag{31}$$

where $\tau = 1 - (1/K_\tau D)$ is a weight factor, with $K_\tau \geq 2$ and D is the number of elements in gradient vector, and the power of the system noise is estimated using longer data as

$$\hat{\sigma}_v^2(k) = \beta\hat{\sigma}_v^2(k-1) + (1-\beta)e_\theta^2(k) \tag{32}$$

with $\beta = 1 - (1/K_\beta D)K_\beta \succ K_\tau$. Now, with $\lambda_k \cong 1$, it leads to $\hat{\sigma}_e(k) \cong \hat{\sigma}_v(k)$. Generally, better estimates are expected with this tuning particularly in signal tracking with step changes of parameters and sudden changes of the network topology and the states. To implement the MGN algorithm, the variables are chosen as follows: $\lambda_1 = 0.55$, $\lambda_2 = 0.55$, and $\widetilde{a}(0) = [1, 0]^T$ for frequency, amplitude, and phase estimation, respectively. The initial amplitude and phase are chosen from some prior knowledge about the signal parameters.

Further, the proposed algorithm can be generalized for multiple harmonic and interharmonic component estimation. For multiple sinusoidal parameter estimation, the discrete-time noisy measurement is given as

$$s(k) = \sum_{r=1}^{R} A_r(k)\sin\left(w_r(k)k + \phi_r(k)\right), \qquad r = 1, 2, \ldots R \tag{33}$$

where A_r, w_r, and ϕ_r are unknown values that denote the amplitude, frequency, and phase of the rth real valued sinusoid, respectively. In a similar way, multifrequency components can be estimated using the procedure outlined in Section III-A. For R sinusoids according to (4), the linear predictor coefficients required are $a_0, a_1, a_2, \ldots, a_{2R}$, with estimation error given in (5). Hence, the parameter vector to be estimated is given by $\widetilde{\theta}(k) = [\widetilde{a}_0 \quad \widetilde{a}_1 \quad \ldots \quad \widetilde{a}_R]^{\mathrm{T}}$, and the updating equation for sinusoidal parameter estimation under noisy condition is as given in (8) and (9), where the gradient vector ψ and the Hessian matrix $H(k)$ [19] are obtained as in (34) and (35), shown at the bottom of the next page

$$\psi(k) = \frac{\partial e_w(k)}{\partial\widetilde{\theta}} = \begin{bmatrix} y(k) + y(k-2R) \\ y(k-1) + y(k-2R+1) \\ y(k-2) + y(k-2R+2) \\ \cdots \\ \cdots \\ \cdots \\ y(k-R+1) + y(k-R-1) \\ y(k-R) \end{bmatrix}. \tag{34}$$

To compute the inverse Hessian matrix, a similar approximation is made to reduce the computational complexity; assuming that w is not near to zero or π, $H(k)$ can be approximated as in (36) and (37), shown at the bottom of the next page. Then, the inverse Hessian matrix is easily calculated as done in Section III-A. Then, the parameters are obtained as in (38), shown at the bottom of the next page, where, the terms $(1,1), (2,2), (3,3), \ldots (R+1, R+1)$ of (37) are denoted as $X1, X2, \ldots X(R+1)$, respectively. Once the frequencies are estimated using (4), amplitude and phase can be estimated as shown in Section III-B, and the amplitude and phase of the harmonics and interharmonics are estimated as

$$\begin{aligned} \hat{A}_r(k) &= \hat{A}_r(k-1) + \sin\left(\hat{w}_r(k-1)k + \hat{\phi}_r(k-1)\right) \\ &\quad \times e_\theta(k)/c(k) \\ \hat{\phi}_r(k) &= \hat{\phi}_r(k-1) + \cos\left(\hat{w}_r(k-1)k + \hat{\phi}_r(k-1)\right) \\ &\quad \times e_\theta(k)/\left(\hat{A}_r(k-1)c(k)\right). \end{aligned} \tag{39}$$

The detail derivation for harmonics, subharmonics, and interharmonics using the proposed algorithm is included in a future paper. One example of harmonic estimation is included in Section IV to show its generalization.

C. Performance Analysis of MGN Algorithm

Here, we will analyze the mean-square estimation errors of the parameters under stationary condition. Thus, let us consider $\theta = [a_0, a_1, A, \phi]^{\mathrm{T}}$, and the covariance matrix in MGN method denoted as $\mathrm{cov}(\hat{\theta}(k))$ is calculated for two different objective functions as

$$\begin{aligned} \mathrm{cov}\left(\hat{\theta}(k)\right) = E\Bigg\{ &\left[\frac{\partial\varepsilon_1^2(k)}{\partial\hat{\theta}^2}\right]^{-1}\left[\frac{\partial\varepsilon_1(k)}{\partial\hat{\theta}}\right] \\ &\times \left[\frac{\partial\varepsilon_1(k)}{\partial\hat{\theta}}\right]^{\mathrm{T}}\left[\frac{\partial\varepsilon_1^2(k)}{\partial\hat{\theta}^2}\right]^{-1}\Bigg\}_{\hat{\theta}(k)=\theta} \end{aligned}$$

$$= \sigma^2 \left[\sum_{i=0}^{k} \lambda_1^{k-i} \psi(i) \psi^{\mathrm{T}}(i) \right]^{-1} \sum_{i=0}^{k} \lambda_1^{2(k-i)} \psi(i) \psi^{\mathrm{T}}(i) \times \left[\sum_{i=0}^{k} \lambda_1^{k-i} \psi(i) \psi^{\mathrm{T}}(i) \right]^{-1} \quad (40)$$

where E denotes the expectation operation. Further, when k is sufficiently large, the covariance reduces to

$$\operatorname{cov}\left(\hat{\theta}(k)\right) \approx \sigma^2 \begin{bmatrix} 1/2c(k)A^2 & 0 \\ 0 & 1/c(k)A^2 \end{bmatrix}. \quad (41)$$

Hence, the variance of the linear predictor coefficients is

$$\operatorname{var}\left(\widetilde{a}_0(k)\right) = \frac{\sigma^2(1-\lambda_1)}{A^2\left(1-\lambda_1^{k+1}\right)} \quad (42)$$

$$\operatorname{var}\left(\widetilde{a}_1(k)\right) = \frac{2\sigma^2(1-\lambda_1)}{A^2\left(1-\lambda_1^{k+1}\right)}. \quad (43)$$

Similarly, analyzing the covariance matrix for the second cost function, the variance of the amplitude and phase are found to be

$$\operatorname{var}\left(\hat{A}(k)\right) = \frac{2\sigma^2(1-\lambda_2)}{\left(1-\lambda_2^{k+1}\right)}$$

$$\operatorname{var}\left(\hat{\phi}(k)\right) = \frac{2\sigma^2(1-\lambda_2)}{A^2\left(1-\lambda_2^{k+1}\right)}. \quad (44)$$

If all the forgetting factors are made equal to unity, then the variances will attain Cramer–Rao lower bound for sufficiently large value of k assuming that the noise $v(k)$ is Gaussian distributed. Hence, it is proven that the MGN algorithm attains optimal performance for stationary amplitude, phase, and frequency in an asymptotic sense. The next section presents computational results for power sinusoids and low-frequency signals.

$$H(k) = \sum_{i=0}^{k} \lambda_1^{k-i} \begin{bmatrix} (y(k)+y(k-2R))^2 & (y(k)+y(k-2R))(y(k-1)+y(k-2R+1)) & \dots & (y(k)+y(k-2R))\,(y(k-R)) \\ (y(k)+y(k-2R))(y(k-1)+y(k-2R+1)) & (y(k-1)+y(k-2R))^2 & \dots & (y(k-1)+y(k-2R))(y(k-R)) \\ \dots & & & \\ \dots & & & \\ \dots & & & \\ \dots & & & \\ (y(k)+y(k-2R))\,(y(k-R)) & (y(k-1)+y(k-2R))\,(y(k-R)) & \dots & (y(k-R))^2 \end{bmatrix} \quad (35)$$

$$H(k) = \sum_{i=0}^{k} \lambda_1^{k-i} \begin{bmatrix} (y(k)+y(k-2R))^2 & 0 & \dots & 0 \\ 0 & (y(k-1)+y(k-2R+1))^2\,0 & \dots & 0 \\ 0 & 0 & (y(k-2)+y(k-2R+2))^2\,0 & 0 \\ \dots & & & \\ \dots & & & \\ \dots & & & \\ 0 & 0 & \dots & (y(k-R))^2 \end{bmatrix} \quad (36)$$

$$H(k) = \frac{1-\lambda_1^{k+1}}{2(1-\lambda_1)} \begin{bmatrix} 2RA_1^2\cos^2(Rw_1)\sin^2\left(w_1(k-R)+\phi_1(k-R)\right) + 8A_2^2\cos^2(Rw_2)\sin^2(w_2(k-R) & & & \\ \quad +\phi_2(k-R)+\ldots+8A_R^2\cos^2(Rw_R)\sin^2\left(w_R(k-R)+\phi_R(k-R)\right) & 0 & \dots & 0 \\ \dots & & & \\ \dots & & & \\ \dots & & & \\ 0 & \dots & 0 & 2A_1^2\sin^2\left(w_1(k-R)+\phi_1(k-R)\right) + A_2^2\sin^2(w_2(k-R) \\ & & & \quad +\phi_2(k-R)+\ldots+A_R^2\sin^2\left(w_R(k-R)+\phi_R(k-R)\right) \end{bmatrix} \quad (37)$$

$$\begin{aligned}
\widetilde{a}_0(k) &= \widetilde{a}_0(k-1) - e_w(k)\left(A_1\cos(Rw_1)\sin\left(w_1(k-R)+\phi_1(k-R)\right) + A_2\cos(Rw_2)\sin\left(w_2(k-R)+\phi_2(k-R)\right)\right. \\
&\quad \left. +\ldots+A_R\cos(Rw_R)\sin\left(w_R(k-R)+\phi_R(k-R)\right)\right)/2Rc(k)X1 \\
\widetilde{a}_1(k) &= \widetilde{a}_1(k-1) - e_w(k)\left(A_1\cos\left((R-1)w_1\right)\sin\left(w_1(k-R)+\phi_1(k-R)\right) + A_2\cos\left((R-1)w_2\right)\sin\left(w_2(k-R)+\phi_2(k-R)\right)\right. \\
&\quad \left. +\ldots+A_R\cos\left((R-1)w_R\right)\sin\left(w_R(k-R)+\phi_R(k-R)\right)\right)/2Rc(k)X2 \\
\widetilde{a}_R(k) &= \widetilde{a}_R(k-1) - e_w(k)\left(A_1\sin\left(w_1(k-R)+\phi_1(k-R)\right) + A_2\sin\left(w_2(k-R)+\phi_2(k-R)\right)\right. \\
&\quad \left. +\ldots+A_R\sin\left(w_R(k-R)+\phi_R(k-R)\right)\right)/2c(k)X(R+1)
\end{aligned} \quad (38)$$

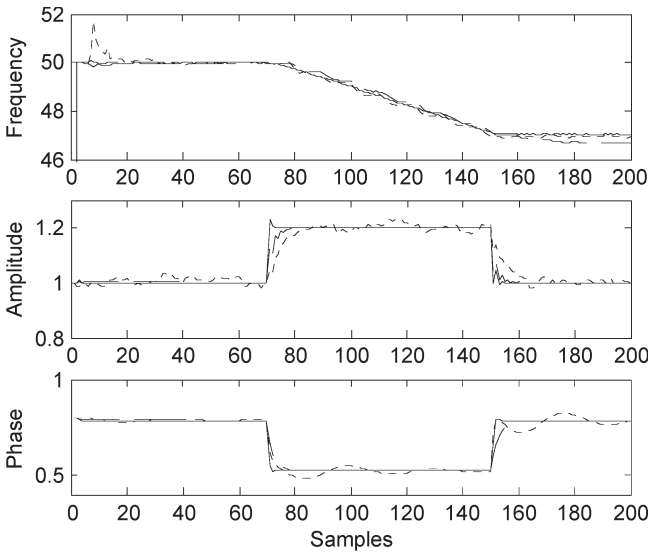

Fig. 1. Estimated frequency, amplitude, and phase at 30-dB noise. (Dotted) EKF. (Dashed) RGN. (Solid) MGN.

IV. Simulation Results

Computer simulations have been carried out to evaluate the performance of the proposed algorithm. The sampling frequency f_s is chosen as 1.6 kHz based on 50-Hz fundamental frequency for cases 1–4 as described hereinafter.

A. Power Signal Analysis

Case 1: This experiment is done for a power signal with a change in signal parameters. The signal is represented as

$$y(k) = A(k)\sin\left(w(k)k + \phi(k)\right) + v_k. \tag{45}$$

For the first 70 samples, $freq = 50$ Hz, $A = 1$ pu, and $\Phi = \tau/4$; for 70–150 samples, the parameter changes to $freq = 47$ Hz, $A = 1.2$ pu, and $\Phi = \tau/6$; and then, it come back to initial values. The angular frequency of the signal is varied as $w(k) = w_0 + (w_1 - w_0)/80(k - 70)$, where $w_0 = 2 * pi * 50/f_s$ and $w_1 = 2 * pi * 47/f_s$, where f_s is the sampling frequency. The signal parameters are estimated using ADALINE [5], extended Kalman filter (EKF) [10], artificial neural network (ANN) [12], LP [15], RGN [18], Hessian matrix approximation [19], and generalized constant modulus algorithm [27], and the proposed method is used for comparison. Out of these, some of the algorithms are used to compute frequency only and some for amplitude and phase. The signal is corrupted with 30-dB noise. The estimated signal parameters using different algorithms are given in Fig. 1. The signal is then tested under different noise levels, and the estimated frequency, amplitude, and phase mean square error in decibels obtained in different algorithms are shown in Fig. 2.

Absolute frequency error, amplitude error, and phase error at different noise levels of different algorithms and their execution times are listed in Table I. Although the ANN algorithm is capable of estimating the harmonics present in the signal, its performance in estimating frequency component deteriorates under high noise condition.

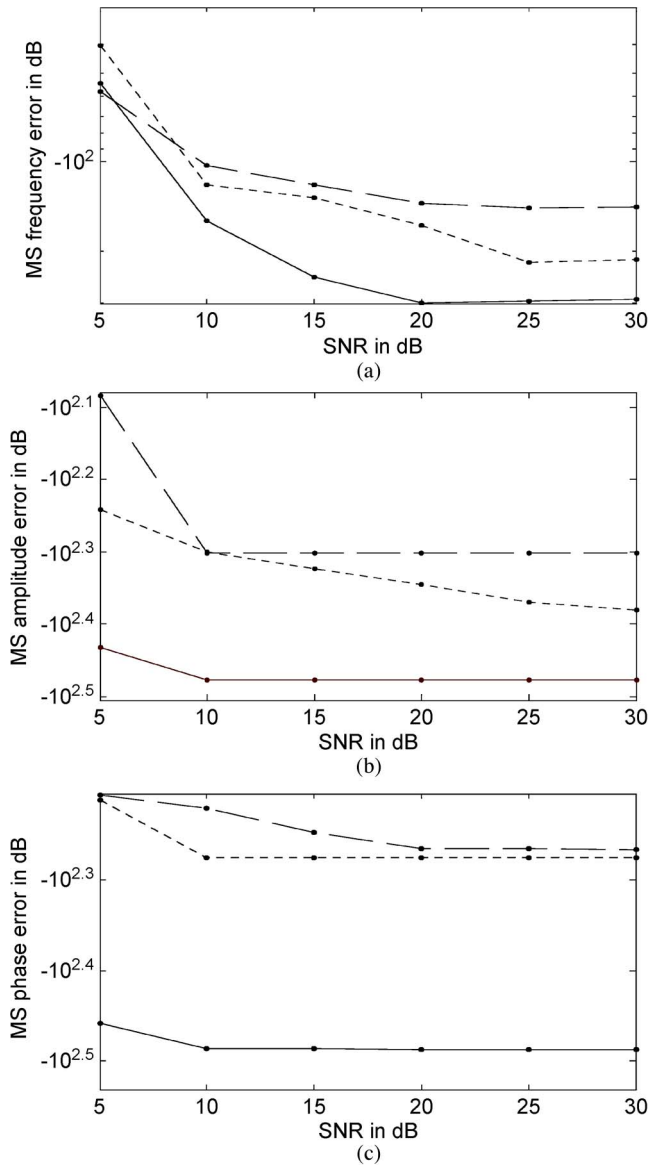

Fig. 2. (a) Mean square frequency error in decibels at different SNR. (b) Mean square amplitude error in decibels at different SNR. (c) Mean square phase error in decibels at different SNR level. (Dashed) EKF. (Dotted) RGN. (Solid) MGN.

Case 2: The second experiment is done for the estimation of a power signal with change in parameters. The signal is represented as in (45). The signal frequency is changed in modulated form as given hereinafter. $w(k) = 2\pi[50 + \sin(2\pi.1.T_s) + .5\sin(2\pi.6.T_s)]$, where T_s is the sampling interval. For the first 70 samples, $A = 1$ pu; for 70–150 samples $A = 0.8$ pu; and then, it comes back to its initial value. Similarly, for the first 50 samples, $\Phi = \pi/4$; for 50–130 samples, $\Phi = \tau/3$; and then, it comes back to its initial value. The signal is corrupted with 30-dB noise. From Fig. 3, it is clear that the proposed algorithm can easily estimate the abruptly changing parameters.

Case 3: The third experiment is done for the estimation of a power signal with change in parameters. The signal is represented as in (45). For the first 250 samples, $freq = 50$ Hz; for 250–400 samples, $freq = 48.5$ Hz; for 400–600 samples, $freq = 51.3$ Hz; and thereafter, $freq = 50$ Hz. Similarly, for the first 150 samples, $A = 1$ pu; for 150–250 samples, $A = 1.2$ pu; and then, it comes back to its initial value.

TABLE I
PERFORMANCE COMPARISON OF DIFFERENT ALGORITHMS

Algorithm	Frequency estimation error (HZ)			Amplitude estimation error (p.u)			Phase estimation error			Execution time (ms)
	30	20	10	30	20	10	30	20	10	
Adaline	0.531	0.713	1.273	0.072	0.915	0.717	0.0097	0.054	0.31	2.19
EKF	0.151	0.202	1.053	0.021	0.039	0.609	0.0063	0.032	0.20	1.53
LP	0.050	0.091	0.201	_	_	_	_	_	_	_
RGN	0.021	0.071	0.103	0.009	0.005	0.034	0.0009	0.003	0.006	0.77
HMA	_	_	_	0.008	0.005	0.30	0.001	0.0033	0.0065	0.58
GCM	_	_	_	0.010	0.006	0.39	0.012	0.0041	0.0069	0.61
ANN	0.036	0.087	0.169	0.007	0.004	0.038	0.0097	0.0052	0.0086	_
MGN(Proposedmethod)	0.001	0.032	0.101	0.007	0.002	0.019	0.0005	0.0001	0.004	0.59

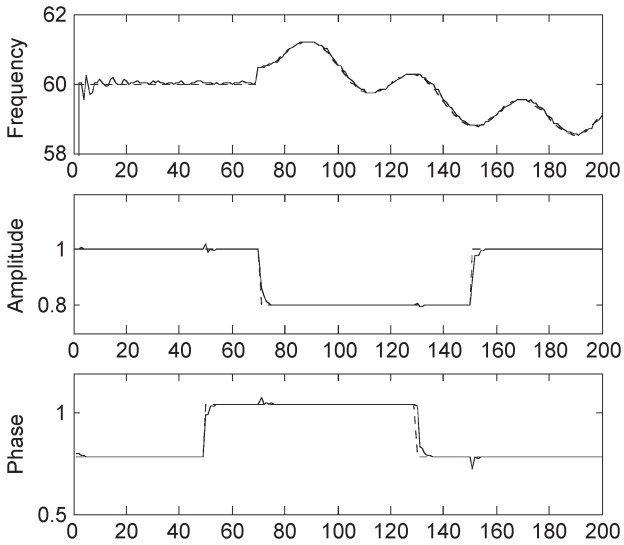

Fig. 3. Estimation of all the signal parameters of case 2. (Dotted) Desired. (Solid) Estimated.

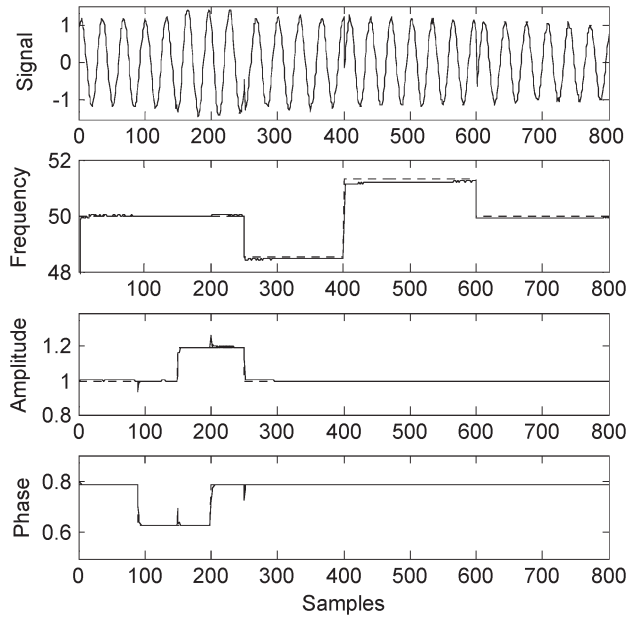

Fig. 4. Estimation of all the signal parameters of case 3. (Dotted) Desired. (Solid) Estimated.

Similarly, for the first 90 samples, $\Phi = \pi/4$; for 90–200 samples, $\Phi = \pi/5$; and then, it comes back to its initial value. The signal is corrupted with 30-dB noise. From Fig. 4, it is clear that the MGN algorithm with adaptive forgetting factor can easily estimate the abrupt change in parameters.

Case 4: The fourth experiment is done for the analysis of the effect of harmonics, interharmonics, and subharmonics as noise on the proposed adaptively tuned MGN algorithm. The test signal is taken as given in (45), and then, the signal is corrupted with 15% third harmonic and 7% fifth harmonic, an interharmonic of 256 Hz, and a subharmonic of 42 Hz. The comparison in error observed for each of the parameter is shown in Fig. 5. From the figure, it is clear that the effect of harmonics, interharmonics, and subharmonics as noise is negligible on the estimation of signal parameters (even with harmonics as noise, the algorithm can easily predict the signal).

The algorithm gives accurate results even for high percentage of harmonics.

Case 5—Damped Sine Wave With Harmonic: The fifth experiment is done for the analysis of the proposed algorithm on a highly distorted sinusoid signal with harmonics and corrupted with 30-dB noise. In case 5 and case 6, the sampling frequency

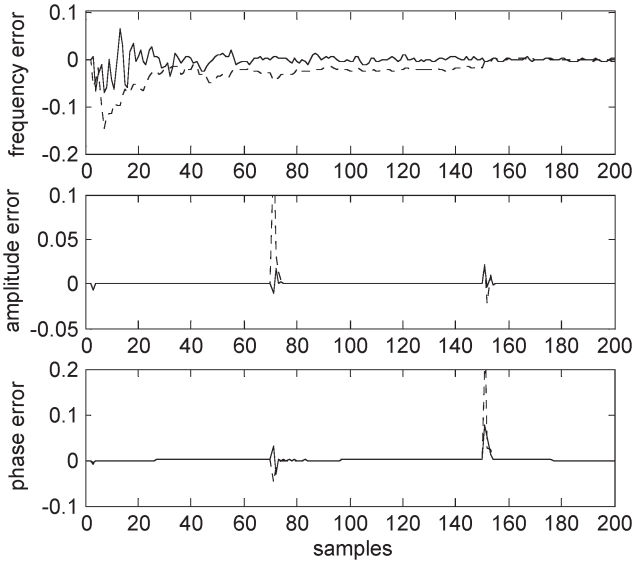

Fig. 5. Estimation error comparison of (solid) signal without harmonics and (dashed) signal with harmonics.

is chosen as 7.2 kHz with a view to compute the highest harmonic component (50th harmonic) if any. The damped sine wave with harmonics is modeled as

$$y(k) = \sum_{n=1}^{9} A_n e^{-(kT_s\alpha)} \sin\left(n\omega_0 kT_s + \phi_n(k)\right) \tag{46}$$

and the parameters are set as the fundamental frequency is 60 Hz, $A1 = 1$ pu, $A3 = 0.7$, $A5 = 0.3$, $A7 = 0.15$, $A9 = 0.05$, $\alpha = 1.5$, $\alpha 3 = \alpha 5 = \alpha 7 = \alpha 9 = 1.5$, $\phi_1 = 0.8$, $\phi_3 = 0.4$, $\phi_5 = 0.7$, $\phi_7 = 0.6$, and $\phi_9 = 0.5$. Fig. 6(a) shows the damped sine wave with harmonics. Fig. 6(b)–(d) shows the fundamental, seventh, and ninth harmonic amplitude and phase components of the estimated signal, respectively. From the figure, it is clear that the proposed algorithm outperforms even for the estimation of such complex signal.

Case-6: The sixth experiment is done for the estimation of the harmonic and interharmonic components. The signal given in (47) is mixed with a noise of $SNR = 30$ dB

$$\begin{aligned} y(k) =& 3\sin(\omega kT_s + \pi/4) + 0.75\sin(7 * \omega kT_s + \pi/6) \\ &+ 0.05\sin(30 * \omega kT_s + \pi/5) \\ &+ 0.5\sin(150 * kT_s + \pi/7) \\ &+ 0.85\sin(498 * kT_s + \pi/4.5) + n_k. \end{aligned} \tag{47}$$

The fundamental frequency of the signal is 60 Hz. Fig. 7(a)–(c) shows the first interharmonic, second interharmonic, and 30th harmonic components of the estimated signal, respectively. From Fig. 7, it is clear that the proposed algorithm can easily and accurately estimate the harmonic and interharmonic components present in the signal.

B. Low-Frequency Signal Analysis

This section presents the estimation of time-varying sinusoid prevalent in communication systems, mechanical systems, vibration strings, biomedical signals, etc. The sampling frequency for low-frequency analysis is chosen as 0.16 kHz.

Case 7: The seventh experiment is done for low-frequency signal analysis. The signal is given as in (45). For the first 70 samples, $freq = 5$ Hz, $A = 1$ pu, and $\Phi = \pi/4$; for 70–150 samples, parameters change to $freq = 5.5$ Hz, $A = 1.2$ pu, and $\Phi = \pi/6$; and then, the parameters come back to initial values. The signal is corrupted with 30-dB noise. From the figure, it is clear that the proposed algorithm can estimate low-frequency signal parameters accurately. The comparison of the MGN algorithm and adaptively tuned MGN is shown in Fig. 8.

C. Experimental Validation

Experimental test data are generated using the laboratory setup, where the load is fed from a 3-kVA 230-V:230-V single-phase transformer, and the data acquisition subsystem is activated using another 230-V:12-V transformer. The voltage across the load after transformation to 12 V is sampled at a rate of 2.0 kHz and is digitized by the A/D system, and the

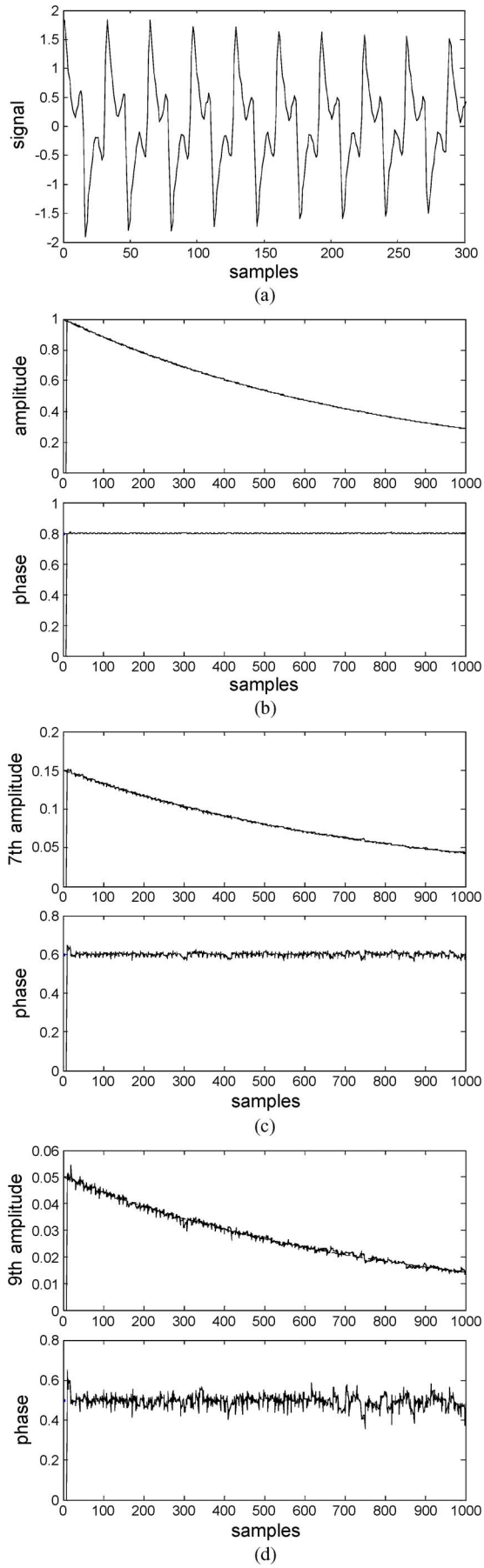

Fig. 6. Estimation of harmonic components in damped sine wave of case 5.

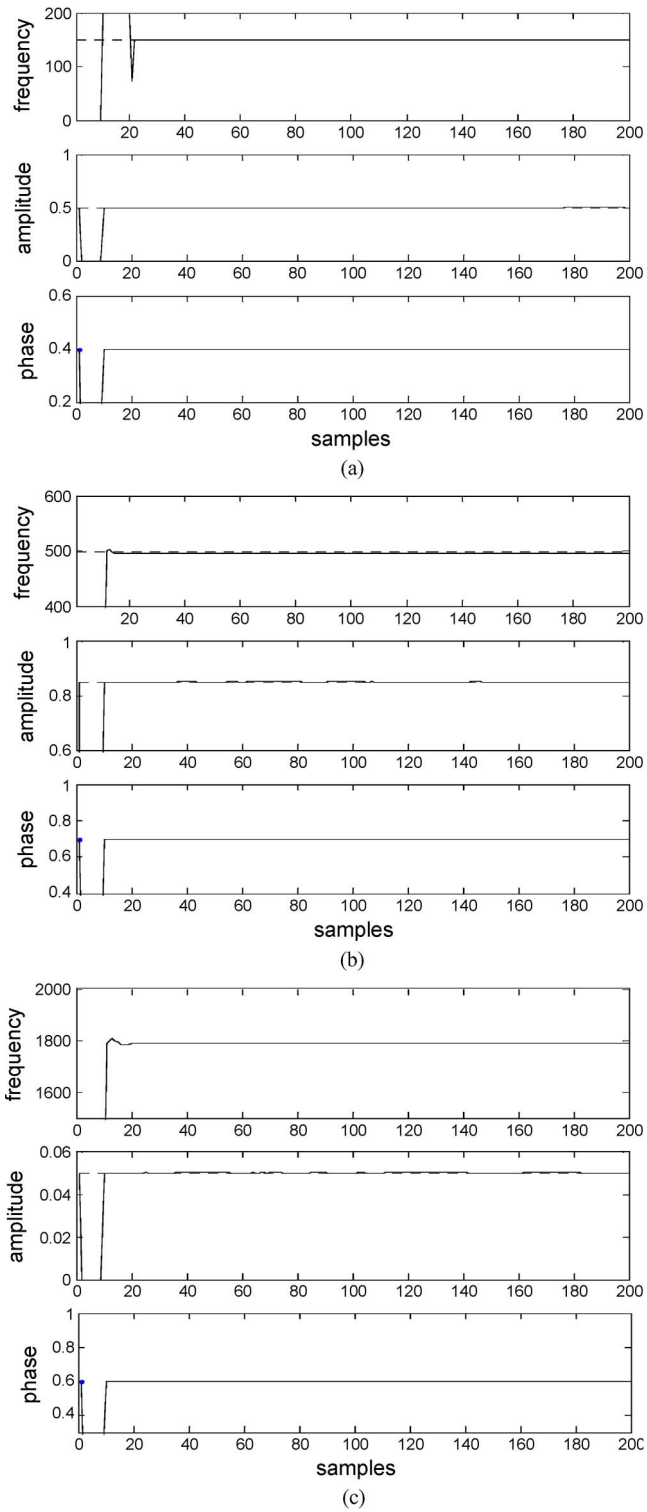

Fig. 7. Estimation of all the parameters of case 6. (Dashed) Desired. (Solid) Tuned MGN algorithm.

digital data are sent to PC using a program written in "C" language. Signals with time-varying amplitude and frequency are obtained using the waveform simulator by switching on and switching off the load, respectively. For frequency estimation, the signal frequency is changed from 10 to 6 Hz and then back to the initial value. Fig. 9 presents the real-time signal estimated using the proposed MGN method.

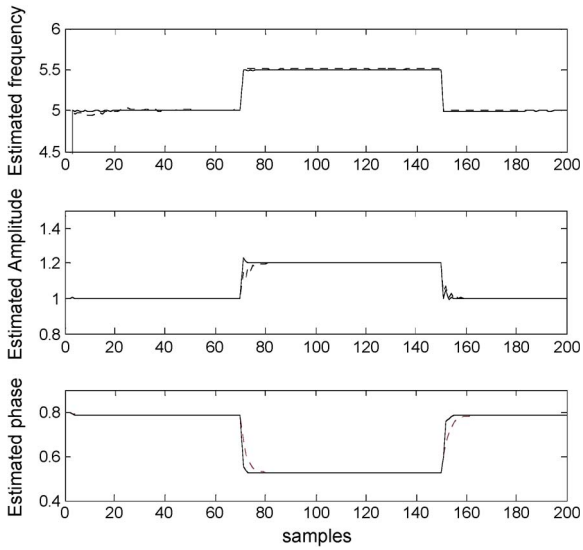

Fig. 8. Estimation of all the parameters of case 7. (Solid) Tuned MGN algorithm and (dashed) MGN algorithm.

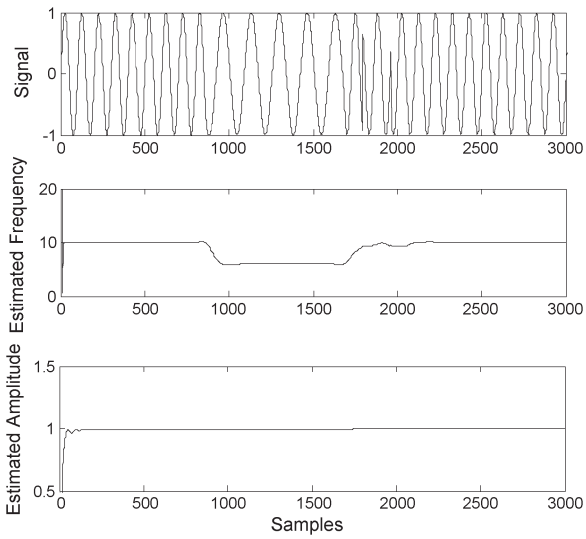

Fig. 9. Real-time test signal with estimated frequency and amplitude.

V. Conclusion

For a time-varying sinusoidal signal, where all the parameters like amplitude, phase, and frequency vary, the proposed algorithm produces the best convergence and least tracking error even in the presence of strong Gaussian white noise with low SNR. To highlight the robust tracking property of the proposed approach, several computational experiments have been presented that include low and power frequencies of a single sinusoid with step changes in amplitude, frequency, and phase. Also, the tracking of damped sinusoids with relatively much less computational burden has been presented with high accuracy. The time required for convergence of the signal parameters to their true values with different SNR is less than a cycle. The analysis presented in this paper for the estimation of time varying amplitude, phase, and frequency of a single sinusoid can be easily used for the calculation of phase and frequency of multiple harmonics, interharmonics, and decaying

dc components in the signal. A harmonic estimation example has also been provided to mark its generalization.

REFERENCES

[1] P. Rodriguez, A. V. Tionbus, R. Teodorescu, M. Liserre, and F. Blaabjerg, "Flexible active power control of distributed generation systems during grid faults," *IEEE Trans. Ind. Electron.*, vol. 54, no. 5, pp. 2583–2592, Oct. 2007.

[2] P. F. Pai, "On-line tracking of instantaneous frequency and amplitude of dynamical system response," *Mech. Syst. Signal Process.*, vol. 24, no. 4, pp. 1007–1024, May 2010.

[3] C. T. Nguyen and K. A. Srinivasan, "A new technique for rapid tracking of frequency deviations based on level crossings," *IEEE Trans. Power App. Syst.*, vol. PAS-103, no. 8, pp. 2230–2236, Aug. 1984.

[4] H. C. Lin and C. S. Lee, "Enhanced FFT-based parameter algorithm for simultaneous multiple harmonics analysis," *Proc. Inst. Elect. Eng.—Gen. Transm. Distrib. Proc.*, vol. 148, no. 3, pp. 209–214, May 2001.

[5] A. K. Pradhan, A. Routray, and A. Basak, "Power system frequency estimation using least mean square technique," *IEEE Trans. Power Del.*, vol. 20, no. 3, pp. 1812–1816, Jul. 2005.

[6] H. C. So, "A comparative study of three recursive least squares algorithms for single-tone frequency tracking," *Signal Process.*, vol. 83, no. 9, pp. 2059–2062, Sep. 2003.

[7] M. Niedzwickei and P. Kaczmarek, "Tracking analysis of a generalized notch filters," *IEEE Trans. Signal Process.*, vol. 54, no. 1, pp. 304–314, Jan. 2006.

[8] V. V. Terzija and V. Stanojevic, "STLS algorithm for power quality indices estimation," *IEEE Trans. Power Del.*, vol. 23, no. 2, pp. 544–552, Apr. 2008.

[9] S. Y. Xue and S. X. Yang, "Power system frequency estimation using supervised Gauss-Newton algorithm," *Measurement*, vol. 42, no. 1, pp. 28–37, Jan. 2009.

[10] C. I. Chen, G. W. Chang, R. C. Hong, and H. M. Li, "Extended real model of Kalman filter for time-varying harmonics estimation," *IEEE Trans. Power Del.*, vol. 25, no. 1, pp. 17–26, Jan. 2010.

[11] C. Huang, C. Lee, K. Shih, and Y. Wang, "Frequency estimation of distorted power system signals using a robust algorithm," *IEEE Trans. Power Del.*, vol. 23, no. 1, pp. 41–51, Jan. 2008.

[12] H. C. Lin, "Intelligent neural network based fast power system harmonic detection," *IEEE Trans. Ind. Electron.*, vol. 54, no. 1, pp. 43–52, Feb. 2007.

[13] G. W. Chang, C.-I. Chen, and Q. W. Liang, "A two-stage adaline for harmonics and interharmonics measurement," *IEEE Trans. Ind. Electron.*, vol. 56, no. 6, pp. 2220–2228, Jun. 2009.

[14] V. L. Pham and K. P. Wong, "Antidistortion method for wavelet transform filter banks and nonstationary power system waveform harmonic analysis," *Proc. Inst. Elect. Eng.—Gen. Transm. Distrib.*, vol. 148, no. 2, pp. 117–122, Mar. 2001.

[15] H. C. So, K. W. Chan, Y. T. Chan, and K. C. Ho, "Linear prediction approach for efficient frequency estimation of multiple sinusoids: Algorithms and analysis," *IEEE Trans. Signal Process.*, vol. 53, no. 7, pp. 2290–2305, Jul. 2005.

[16] Z. G. Zhang, S. C. Chan, and K. M. Tsui, "A recursive frequency estimation using linear prediction and a Kalman filter based iterative algorithm," *IEEE Trans. Circuits Syst. II, Exp. Briefs*, vol. 55, no. 6, pp. 576–580, Jun. 2008.

[17] H. Fu and P. Kam, "MAP/ML estimation of the frequency and phase of a signal sinusoid in noise," *IEEE Trans. Signal Process.*, vol. 55, no. 3, pp. 834–845, Mar. 2007.

[18] J. Yang, H. Xi, and W. Guo, "Robust modified newton algorithm for adaptive frequency estimation," *IEEE Signal Process. Lett.*, vol. 14, no. 11, pp. 879–882, Nov. 2007.

[19] J. Zheng, K. W. K. Lui, W. K. Ma, and H. C. So, "Two simplified recursive Gauss–Newton algorithms for direct amplitude and phase tracking of a real sinusoid," *IEEE Signal Process. Lett.*, vol. 14, no. 12, pp. 972–975, Dec. 2007.

[20] R. Zivanovic, "An adaptive differentiation filter for tracking instantaneous frequency in power systems," *IEEE Trans. Power Del.*, vol. 22, no. 2, pp. 765–771, Apr. 2007.

[21] H. C. Lin, "Fast tracking of time-varying power system frequency and harmonics using iterative-loop approaching algorithm," *IEEE Trans. Ind. Electron.*, vol. 54, no. 2, pp. 974–983, Apr. 2007.

[22] H. E. P. de Souza, F. Bradaschia, F. A. S. Neves, M. C. Cavalcanti, G. M. S. Azevedo, and J. P. de Aruda, "A method for extracting the fundamental frequency, positive sequence voltage vector based on simple mathematical transformations," *IEEE Trans. Ind. Electron.*, vol. 56, no. 5, pp. 1539–1547, May 2009.

[23] D. Yazdani, A. Bakhshai, G. Joos, and M. Mojiri, "A real-time extraction of harmonic and reactive current in nonlinear load for grid-connected converters," *IEEE Trans. Ind. Electron.*, vol. 56, no. 6, pp. 2185–2189, Jun. 2009.

[24] M. D. Kusljevic, "A simple recursive algorithm for simultaneous magnitude and frequency estimation," *IEEE Trans. Instrum. Meas.*, vol. 57, no. 6, pp. 1207–1214, Jun. 2008.

[25] R. A. Zadeh, A. Ghosh, G. Ledwitch, and F. Zare, "Analysis of phasor measurement method in tracking power system frequency of distorted signals," *IET Gen. Transm. Distrib.*, vol. 4, no. 7, pp. 759–769, Jul. 2010.

[26] C. Paleologan, J. Benesty, and S. Ciochina, "A robust variable forgetting factor recursive least-squares algorithm for system identification," *IEEE Signal Process. Lett.*, vol. 15, pp. 597–600, 2008.

[27] X.-L. Li and X.-D. Zhang, "On the tracking performance of a family of generalized constant modulus algorithm," in *Proc. IEEE ICASSP*, Apr. 2007, vol. III, pp. III-125–III-128.

P. K. Dash (SM'90–LSM'09) received the B.E., M.E., Ph.D., and D.Sc. degrees in electrical engineering in 1962, 1964, 1972, and 2003, respectively, and the Postdoctoral fellowship from the University of Calgary, Calgary, AB, Canada in 1975.

He is the Director in research and consultancy with multidisciplinary research cell, Siksha O Anusandhan University, Bhubaneswar, India. His research interests are in the area of power quality, FACTS, soft computing, deregulation and energy markets, signal processing, and data mining and control.

Dr. Dash is a Fellow of the Indian National Academy of Engineering.

Shazia Hasan (M'11) received the B.E. degree in electronics and telecommunication engineering from the University College of Engineering, Burla, India, in 2002.

She is an Assistant Professor with the Department of Instrumentation and Control, Institute of Technical Education and Research, Siksha O Anusandhan University, Bhubaneswar, India. Her area of interest includes digital signal processing and its application to power system.